

A New Robust Adaptive Beamforming Algorithm Based on GSC

Xiaohan Guan, Yao Chen*, and Encheng Wang

North China University of Technology, No. 5 Jinyuanzhuang Road, Shijingshan District, Beijing, China

ABSTRACT: The generalized sidelobe cancellation (GSC) is a commonly used adaptive beamforming technology, which can be used in antenna arrays. Due to the error of the direction of arrival of the received signal and the spacing error of the received array elements, the signal received by the array antenna has a mismatch of steering vectors, which leads to that the GSC method cannot accurately aim at the expected signal and suppress the interference signal. In order to improve the robustness of GSC algorithm, a new adaptive beamforming algorithm named SGSC (Sequential Quadratic Programming-Generalized Side Lobe Cancellation) is proposed in this paper. In this method, firstly, the mismatching expected signal steering vector is corrected by the stepwise quadratic programming, so that the auxiliary antenna can effectively block the expected signal. Then, the optimal weight vector is obtained by combining the corrected steering vector with the GSC, so that the expected signal components of the auxiliary antenna and of the main antenna can be avoided from being cancelled due to mismatch errors. Finally, the simulation results based on MATLAB show that the new algorithm can point the desired signal more accurately and suppress the interference signal more obviously in the presence of mismatch error, which shows the effectiveness of the method.

1. INTRODUCTION

Nowadays, adaptive beamforming technology has been widely used in navigation, communication, and other scientific and technological fields. One of its main tasks is to form null in the interference direction to suppress interference and form main beam in the desired signal direction [1–3]. Due to the sensitivity of the adaptive beamformer, when the model is mismatched, that is, the expected signal exists in the training data, or steering vector is mismatched, the performance of the traditional adaptive beamformer is seriously degraded [4–7]. Therefore, improving the robustness of adaptive beamforming has always been a subject that needs in-depth study.

At present, robust adaptive beamforming techniques can be divided into two categories according to model mismatch. The first kind is to deal with the situation that the expected signal exists in the training data. At this time, the accurate interference noise covariance matrix (INCM) cannot be obtained, so the robustness of the algorithm can be improved by reconstructing the INCM. The second is to deal with the mismatch of steering vectors. Because the direction of the expected signal cannot be accurately obtained, the sensitivity of the beamformer to mismatch errors can be reduced by correcting the steering vectors of the expected signal.

Reference [8] reconstructed the INCM by Capon spectrum integration without noise power, but it is easily influenced by the sensitivity of spectrum to the random error of steering vector. Reference [9] constructed a selection matrix that can determine the eigenvectors and eigenvalues corresponding to the desired signal, and then determines INCM according to the size of the selected eigenvalues. However, the selection of the target signal is uncertain. Reference [10] estimated the values of steering vector and INCM through sparse reconstruction, and

then established a constraint model based on subspace expansion to optimize steering vector and INCM, and finally obtained the optimal weight vector, but this method is suitable for a specific error mismatch. The above literatures all use INCM reconstruction method to improve the robustness of the algorithm. Because GSC (Generalized Side Lobe Cancellation) algorithm is not suitable for complex environment, some literatures have proposed some robust beamforming algorithms based on GSC algorithm. Reference [11] used zero-widened blocking matrix to filter out the signal components in the auxiliary channel of GSC, which can improve the robustness of GSC algorithm when the signal steering vector is mismatched, but this method requires complex calculation. Reference [12] used the method of covariance matrix taper to add virtual interference to the snapshot number to obtain a GSC zero widening method with high computational efficiency, which requires less computation. Reference [13] proposed a near-channel subtraction scheme to improve the block matrix of GSC to improve the performance of GSC algorithm Generalized Side Lobe Cancellation. However, the above two methods are not suitable for various mismatch errors. In [14], the least mean square algorithm was used to estimate the noise component in the output signal of GSC, and then the estimated noise component was subtracted to improve the denoising performance of GSC, which can reduce the distortion under the condition of large noise direction error. However, this method cannot deal with the mismatch of steering vectors.

Based on the above methods, this paper proposes a new robust adaptive beamforming algorithm, which combines the stepwise quadratic programming method with the GSC algorithm. The proposed method uses the stepwise quadratic programming method to correct the steering vector of the expected signal, so that the auxiliary antenna can effectively block the ex-

* Corresponding author: Yao Chen (1730869912@qq.com).

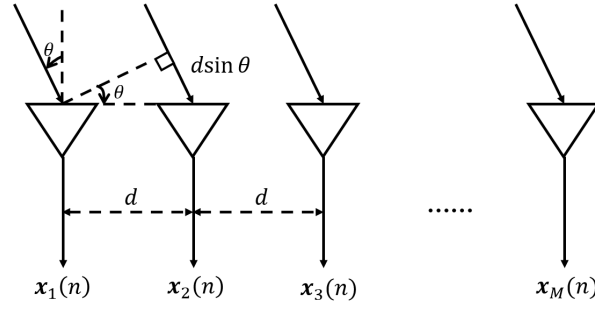


FIGURE 1. Array signal receiving model.

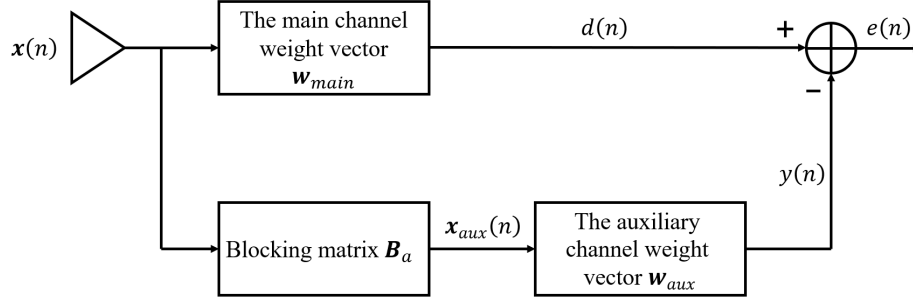


FIGURE 2. Generalized sidelobe cancellation system.

pected signal, thus reducing the adverse impact of the steering vector on the GSC algorithm. Compared with the conventional GSC algorithm, this method can more accurately align the desired signal and suppress the interference signal in the presence of mismatch error, and improve the robustness of the algorithm against steering vector mismatch.

2. THE CONVENTIONAL GSC MODEL

Consider that the array signal receiving model is composed of a uniform linear array (ULA) consisting of m array elements, as shown in Fig. 1. Assuming that both the desired signal and interference signal are far-field narrow-band signals, the array elements are equally spaced. The array element spacing is D , and the incident angle of the signal is θ . The steering vector of the signal is

$$\mathbf{a}(\theta) = [1, e^{-j\varphi}, e^{-j2\varphi}, \dots, e^{-j(M-1)\varphi}]^T \quad (1)$$

where $\varphi = 2\pi d \sin \theta / \lambda$, λ is the wavelength of the signal, and it is twice the array element spacing d , that is $d/\lambda = 0.5$.

When there are $K + 1$ signals incident on the linear array from different directions, the signals received by the linear array are [15, 16]

$$\begin{aligned} \mathbf{x}(n) &= \mathbf{a}(\theta_0) s_0(n) + \sum_{k=1}^K \mathbf{a}(\theta_k) s_k(n) + \mathbf{v}(n) \\ &= \mathbf{a}(\theta_0) s_0(n) + \mathbf{A}_j \mathbf{s}_j(n) + \mathbf{v}(n) \end{aligned} \quad (2)$$

where $s_0(n)$ is the expected signal from θ_0 direction; $\mathbf{a}(\theta_0)$ is the steering vector corresponding to the ex-

pected signal; $s_k(n)$ is K uncorrelated interference signals and $K = 1, 2, \dots, K$, which can also be expressed as $\mathbf{s}_j(n) = [s_1(n), s_2(n), \dots, s_K(n)]^T$; $\mathbf{a}(\theta_k)$ is the steering vector corresponding to the interference signal, which can be represented by the matrix $\mathbf{A}_j = [\mathbf{a}(\theta_1), \dots, \mathbf{a}(\theta_K)]$; so the interference signal component can be represented by $\mathbf{A}_j \mathbf{s}_j(n)$. $\mathbf{v}(n)$ is the Gaussian white noise with power σ_n^2 .

If the steering vector matrix $\mathbf{A} = [\mathbf{a}(\theta_0), \mathbf{a}(\theta_1), \dots, \mathbf{a}(\theta_K)]$ is defined, the linear array received signal can also be expressed as [17–20]

$$\mathbf{x}(n) = \mathbf{A} \mathbf{s}(n) + \mathbf{v}(n) \quad (3)$$

where $\mathbf{s}(n) = [s_0(n), s_1(n), s_2(n), \dots, s_K(n)]^T$.

The GSC transforms the received array signal containing the expected signal direction information into two branches, which are divided into an upper branch and a lower branch, namely a main channel and an auxiliary channel. The system structure is shown in Fig. 2. The signal received by the main antenna at time n can be expressed as

$$\mathbf{x}_{main}(n) = \mathbf{x}(n) = \mathbf{A}_{main} \mathbf{s}(n) + \mathbf{v}_{main}(n) \quad (4)$$

where \mathbf{A}_{main} represents the steering vector corresponding to the signal received by the main antenna, and \mathbf{v}_{main} represents the noise vector in the main antenna. The signal received by the auxiliary antenna at time n is expressed as

$$\mathbf{A}_{aux}(n) = \mathbf{A}_{aux} \mathbf{s}(n) + \mathbf{v}_{aux}(n) \quad (5)$$

where \mathbf{A}_{aux} represents the steering vector corresponding to the signal received by the auxiliary antenna, and \mathbf{v}_{aux} represents the noise vector in the auxiliary antenna.

\mathbf{B}_a shown in Fig. 2 is an auxiliary channel blocking matrix, which is used to eliminate the signal in the main lobe direction

and prevent it from entering the auxiliary channel, so the array signal $\mathbf{x}_{aux}(n)$ can be expressed as,

$$\mathbf{x}_{aux}(n) = \mathbf{B}_a \mathbf{x}(n) = \mathbf{B}_a \mathbf{x}_{main}(n) = \mathbf{B}_a \mathbf{a}(\theta_0) s_0(n) + \mathbf{B}_a \mathbf{z}(n) \quad (6)$$

where $\mathbf{z}(n) = \mathbf{A}_j \mathbf{s}_j(n) + \mathbf{v}(n)$ are interference and noise components.

\mathbf{w}_{main} is the main channel weight vector, and at time n , $\mathbf{x}_{main}(n)$ is obtained by weighting the fixed weight vector \mathbf{w}_{main} .

$$d(n) = \mathbf{w}_{main}^H \mathbf{x}_{main}(n) = \mathbf{w}_{main}^H \mathbf{a}(\theta_0) s_0(n) + \mathbf{w}_{main}^H \mathbf{z}(n) \quad (7)$$

$\mathbf{w}_{main}^H \mathbf{z}(n)$ indicates the interference and noise components that need to be suppressed. In order to suppress the interference plus noise component $\mathbf{w}_{main}^H \mathbf{z}(n)$ and avoid the cancellation of the main lobe expected signal component as much as possible, the output $y(n)$ of the auxiliary channel should not contain the expected signal, so when the received signal passes through the auxiliary channel with the function of blocking the expected signal, the blocking matrix $\mathbf{B}_a \in \mathbb{C}^{M \times M}$ of blocking the desired signal satisfies [21, 22]

$$\mathbf{B}_a \mathbf{a}(\theta_0) = 0 \quad (8)$$

At this time, the array signal $\mathbf{x}_{aux}(n)$ is only related to interference and noise components, that is

$$\mathbf{x}_{aux}(n) = \mathbf{B}_a \mathbf{z}(n) \quad (9)$$

The weight vector of the auxiliary channel can be solved by the principle of MMSE (minimum mean square error), which should minimize the mean square error value of the output, that is

$$\min_{\mathbf{w}_{aux}} |d(n) - \mathbf{w}_{aux}^H \mathbf{x}_{aux}(n)|^2 \quad (10)$$

Therefore, the optimal weighting coefficient can be solved

$$\mathbf{w}_{aux} = \mathbf{R}_x^{-1} \mathbf{R}_{xd} \quad (11)$$

where $\mathbf{R}_x = E\{\mathbf{x}_{aux}(n) \mathbf{x}_{aux}^H(n)\}$ and $\mathbf{R}_{xd} = E\{\mathbf{x}_{aux}(n) d^*(n)\}$, so the expansion of formula (11) can be obtained

$$\begin{aligned} \mathbf{w}_{aux} &= \mathbf{R}_x^{-1} \mathbf{R}_{xd} = (\mathbf{x}_{aux}(n) \mathbf{x}_{aux}^H(n))^{-1} (\mathbf{x}_{aux}(n) d^*(n)) \\ &= (\mathbf{B}_a \mathbf{x}(n) \mathbf{x}^H(n) \mathbf{B}_a^H)^{-1} (\mathbf{B}_a \mathbf{x}(n) \mathbf{x}^H(n) \mathbf{w}_{main}) \\ &= (\mathbf{B}_a \mathbf{R}_{xx} \mathbf{B}_a^H)^{-1} (\mathbf{B}_a \mathbf{R}_{xx} \mathbf{w}_{main}) \end{aligned} \quad (12)$$

where $\mathbf{R}_{xx} = E[\mathbf{x}(n) \mathbf{x}^H(n)]$ represents the autocorrelation matrix of the received signal. After weighting $\mathbf{x}_{aux}(n)$ with auxiliary channel weight vector \mathbf{w}_{aux} , the output can be obtained

$$y(n) = \mathbf{w}_{aux}^H \mathbf{x}_{aux}(n) = \mathbf{w}_{aux}^H \mathbf{B}_a \mathbf{z}(n) \quad (13)$$

The output error can be obtained by subtracting the array signals of the main channel weighted by the weight vector and the auxiliary channel weighted by the weight vector

$$e(n) = d(n) - y(n) = (\mathbf{w}_{main}^H - \mathbf{w}_{aux}^H \mathbf{B}_a) \mathbf{x}(n) \quad (14)$$

The optimal weight vector of the beamforming algorithm of the whole GSC is

$$\mathbf{w}_{GSC} = \mathbf{w}_{main} - \mathbf{B}_a^H \mathbf{w}_{aux} \quad (15)$$

where \mathbf{w}_{main} is usually replaced by $\mathbf{a}(\theta_0)$, that is

$$\mathbf{w}_{GSC} = \mathbf{a}(\theta_0) - \mathbf{B}_a^H (\mathbf{B}_a \mathbf{R}_{xx} \mathbf{B}_a^H)^{-1} \mathbf{B}_a \mathbf{R}_{xx} \mathbf{a}(\theta_0) \quad (16)$$

In practical application, the actual arrival direction of the expected signal is not accurate, that is, there is a mismatching error of the steering vector.

3. CORRECTION OF EXPECTED SIGNAL STEERING VECTOR BY STEPWISE QUADRATIC METHOD

The existence of mismatch error will make $\mathbf{B}_a \mathbf{a}(\theta_0) \neq 0$. At this time, the blocking matrix cannot effectively block the expected signal, and the signal output by the auxiliary channel will contain signal components that cancel the expected signal in the main channel, resulting in the performance degradation of the algorithm. Therefore, this paper uses the method based on stepwise quadratic programming to correct the steering vector of the expected signal, so as to reduce the adverse influence of the steering vector on the GSC algorithm.

In practical application, the real steering vector $\mathbf{a}(\theta_0)$ is difficult to get directly, so the assumed steering vector $\bar{\mathbf{a}}(\theta_0)$ is used to calculate. In order to make the assumed steering vector closer to the real steering vector, the assumed expected signal steering vector $\bar{\mathbf{a}}(\theta_0)$ is corrected with the steering mismatch error vector \mathbf{e} , and in order to reduce the mismatch error between $\mathbf{a}(\theta_0)$ and $\bar{\mathbf{a}}(\theta_0)$, this paper uses the method of stepwise quadratic programming to correct the mismatch error, as shown in Fig. 3.

As can be seen from Fig. 3, firstly, the expected signal steering vector with mismatch error is corrected by the stepwise quadratic programming method, and the corrected expected signal steering vector is substituted into the ideal generalized sidelobe cancellation algorithm to obtain new main channel weight vectors and auxiliary channel weight vectors, so as to obtain signals output from the main channel and auxiliary channel, respectively. The error vector \mathbf{e} can be solved by maximizing the output power value, and its optimization problem is expressed as

$$\begin{aligned} \min_{\mathbf{e}} (\bar{\mathbf{a}}(\theta_0) + \mathbf{e})^H \hat{\mathbf{R}}_{xx}^{-1} (\bar{\mathbf{a}}(\theta_0) + \mathbf{e}) \\ \text{s.t. } \|\bar{\mathbf{a}}(\theta_0) + \mathbf{e}\| = \sqrt{M} \end{aligned} \quad (17)$$

where $\hat{\mathbf{R}}_{xx} = \frac{1}{N} \sum_{n=1}^N \mathbf{x}(n) \mathbf{x}^H(n)$ represents the sample covariance matrix of the received signal, and N is the N snapshot sampling data of the received signal.

In order to transform the non-convex problem of Equation (17) into a convex optimization problem, two mutually orthogonal subspaces are first established

$$\begin{aligned} \mathbf{A}_1 &\triangleq \int_{\Theta} \mathbf{a}(\theta) \mathbf{a}(\theta)^H d\theta \\ \mathbf{A}_2 &\triangleq \int_{\bar{\Theta}} \mathbf{a}(\theta) \mathbf{a}(\theta)^H d\theta \end{aligned} \quad (18)$$

where $\mathbf{a}(\theta)$ is the steering vector in the θ direction, Θ the angle interval of all possible arrival directions of the desired signal, and $\bar{\Theta}$ the complement of Θ . The matrix \mathbf{A}_1 is decomposed into

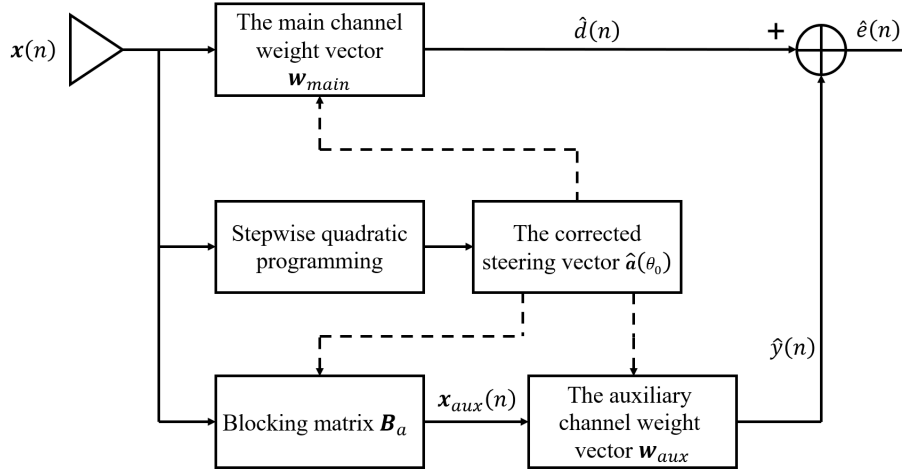


FIGURE 3. Block diagram of generalized sidelobe cancellation after vector correction.

features, and the Q largest eigenvalues are taken out to form a diagonal matrix $\Lambda_1 = \text{diag}(\lambda_1, \lambda_2, \dots, \lambda_Q) \in \mathbf{A}_1^{Q \times Q}$. The eigenvectors $\mathbf{v}_1, \mathbf{v}_2, \dots, \mathbf{v}_Q$ correspond to these Q eigenvalues form the matrix $\mathbf{V}_1 = [\mathbf{v}_1, \mathbf{v}_2, \dots, \mathbf{v}_Q] \in \mathbf{A}_1^{M \times Q}$. Take out the remaining eigenvalues to form diagonal matrix $\Lambda_2 = \text{diag}(\lambda_{Q+1}, \lambda_{Q+2}, \dots, \lambda_M) \in \mathbf{A}_1^{(M-Q) \times (M-Q)}$, and their corresponding eigenvectors $\mathbf{v}_{Q+1}, \mathbf{v}_{Q+2}, \dots, \mathbf{v}_M$ form a matrix $\mathbf{V}_2 = [\mathbf{v}_{Q+1}, \mathbf{v}_{Q+2}, \dots, \mathbf{v}_M] \in \mathbf{A}_1^{M \times (M-Q)}$. At this time, there is

$$\mathbf{A}_1 = \mathbf{V}_1 \Lambda_1 \mathbf{V}_1^H + \mathbf{V}_2 \Lambda_2 \mathbf{V}_2^H \quad (19)$$

The actual steering vector $\mathbf{a}(\theta_0) = \bar{\mathbf{a}}(\theta_0) + \mathbf{e}$ can be expressed linearly by the column vector in \mathbf{V}_1 . In addition, by constructing the projection matrix $\mathbf{P} \triangleq \mathbf{I} - \mathbf{V}_1 \mathbf{V}_1^H$ orthogonal to the desired signal subspace, there is $\mathbf{P}(\bar{\mathbf{a}}(\theta_0) + \mathbf{e}) = 0$, so the optimization problem can be written as follows

$$\begin{aligned} \min_{\mathbf{e}} & (\bar{\mathbf{a}}(\theta_0) + \mathbf{e})^H \hat{\mathbf{R}}_{xx}^{-1} (\bar{\mathbf{a}}(\theta_0) + \mathbf{e}) \\ \text{s.t. } & \mathbf{P}(\bar{\mathbf{a}}(\theta_0) + \mathbf{e}) = 0, \quad \|\bar{\mathbf{a}}(\theta_0) + \mathbf{e}\| = \sqrt{M} \end{aligned} \quad (20)$$

Then the error vector \mathbf{e} is decomposed into a part \mathbf{e}_\perp perpendicular to a $\bar{\mathbf{a}}(\theta_0)$ and a part \mathbf{e}_\parallel parallel to $\bar{\mathbf{a}}(\theta_0)$. In order to estimate \mathbf{e} , we only need to solve the part \mathbf{e}_\perp perpendicular to $\bar{\mathbf{a}}(\theta_0)$, and in order to ensure that the modified steering vector has the same modulus as the assumed expected signal steering vector, the optimization problem can be written as follows

$$\begin{aligned} \min_{\mathbf{e}_\perp} & (\bar{\mathbf{a}}(\theta_0) + \mathbf{e}_\perp)^H \hat{\mathbf{R}}_{xx}^{-1} (\bar{\mathbf{a}}(\theta_0) + \mathbf{e}_\perp) \\ \text{s.t. } & \mathbf{P}(\bar{\mathbf{a}}(\theta_0) + \mathbf{e}_\perp) = 0, \\ & \|\bar{\mathbf{a}}(\theta_0) + \mathbf{e}_\perp\| \leq \sqrt{M} + \delta, \\ & \bar{\mathbf{a}}^H(\theta_0) \mathbf{e}_\perp = 0 \end{aligned} \quad (21)$$

where $\delta > 0$ is a tiny quantity. Considering that the solution of Equation (21) will amplify the noise power in

the case of low signal-to-noise ratio, the signal constraint $(\bar{\mathbf{a}}(\theta_0) + \mathbf{e}_\perp)^H \tilde{\mathbf{C}} (\bar{\mathbf{a}}(\theta_0) + \mathbf{e}_\perp) \leq \bar{\mathbf{a}}^H(\theta_0) \tilde{\mathbf{C}} \bar{\mathbf{a}}(\theta_0)$ is added to suppress the output power of sidelobes. Finally, Equation (21) will be optimized

$$\begin{aligned} \min_{\mathbf{e}_\perp} & (\bar{\mathbf{a}}(\theta_0) + \mathbf{e}_\perp)^H \hat{\mathbf{R}}_{xx}^{-1} (\bar{\mathbf{a}}(\theta_0) + \mathbf{e}_\perp) \\ \text{s.t. } & \mathbf{P}(\bar{\mathbf{a}}(\theta_0) + \mathbf{e}_\perp) = 0, \\ & \|\bar{\mathbf{a}}(\theta_0) + \mathbf{e}_\perp\| \leq \sqrt{M} + \delta, \\ & \bar{\mathbf{a}}^H(\theta_0) \mathbf{e}_\perp = 0, \\ & (\bar{\mathbf{a}}(\theta_0) + \mathbf{e}_\perp)^H \tilde{\mathbf{C}} (\bar{\mathbf{a}}(\theta_0) + \mathbf{e}_\perp) \leq \bar{\mathbf{a}}^H(\theta_0) \tilde{\mathbf{C}} \bar{\mathbf{a}}(\theta_0) \end{aligned} \quad (22)$$

Using iterative method, the vector \mathbf{e}_\perp is updated continuously until the vector \mathbf{e}_\perp satisfies $(\bar{\mathbf{a}}(\theta_0) + \mathbf{e}_\perp)^H \hat{\mathbf{R}}_{xx}^{-1} (\bar{\mathbf{a}}(\theta_0) + \mathbf{e}_\perp) \geq \bar{\mathbf{a}}^H(\theta_0) \hat{\mathbf{R}}_{xx}^{-1} \bar{\mathbf{a}}(\theta_0)$, so that the corrected expected signal steering vector is as close as possible to the actual expected signal steering vector. In order to ensure the modulus consistency, the modulus of the solved expected signal steering vector is corrected to obtain the estimated expected signal steering vector as follows

$$\hat{\mathbf{a}}(\theta_0) = \left(\sqrt{M} / \|\bar{\mathbf{a}}(\theta_0) + \mathbf{e}_\perp\| \right) (\bar{\mathbf{a}}(\theta_0) + \mathbf{e}_\perp) \quad (23)$$

By substituting this modified steering vector into Equation (16), the optimal weight vector of robust beamforming algorithm based on GSC can be obtained,

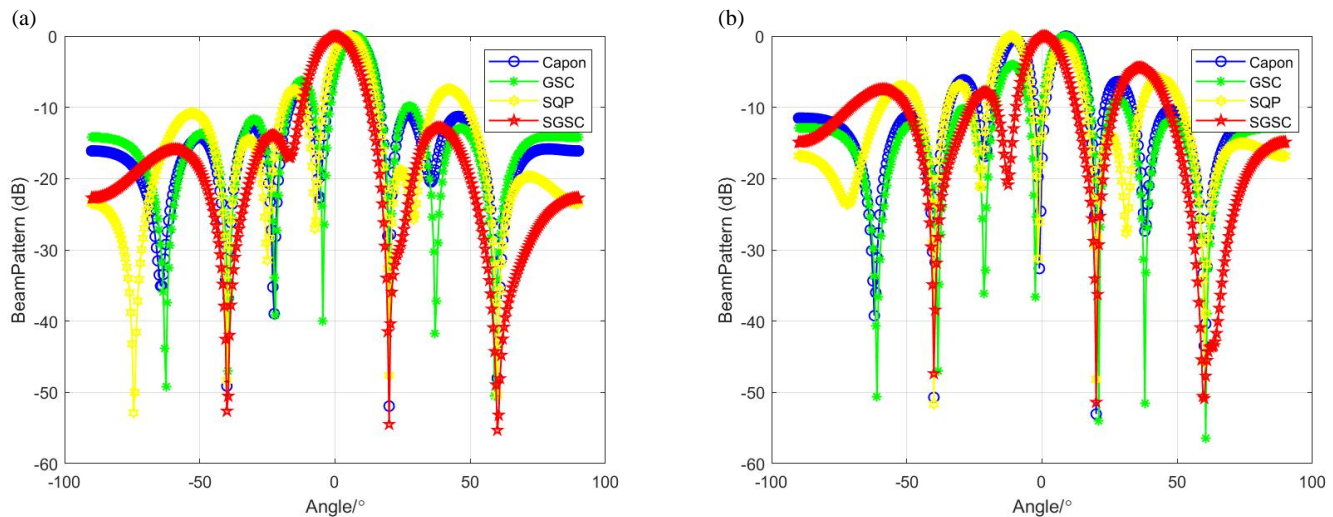
$$\hat{\mathbf{w}}_{GSC} = \hat{\mathbf{a}}(\theta_0) - \mathbf{B}_a^H (\mathbf{B}_a \mathbf{R}_{xx} \mathbf{B}_a^H)^{-1} \mathbf{B}_a \mathbf{R}_{xx} \hat{\mathbf{a}}(\theta_0) \quad (24)$$

At this time, the array signals of the main channel and the auxiliary channel weighted by the modified weight vector are subtracted to obtain the output error,

$$\begin{aligned} \hat{e}(n) &= \hat{d}(n) - \hat{y}(n) = \hat{\mathbf{w}}_{GSC}^H \mathbf{x}(n) \\ &= \left(\hat{\mathbf{a}}(\theta_0) - \mathbf{B}_a^H (\mathbf{B}_a \mathbf{R}_{xx} \mathbf{B}_a^H)^{-1} \mathbf{B}_a \mathbf{R}_{xx} \hat{\mathbf{a}}(\theta_0) \right)^H \mathbf{x}(n) \end{aligned} \quad (25)$$

TABLE 1. Array signal receiving model.

Parameter type	Parameter setting	Parameter type	Parameter setting
Formation	8-element linear array	Interference 1INR	20 dB
Array element spacing	Half wavelength	Interference 2#direction	20 degree
Interference type	White Gaussian noise	Interference 2#INR	20 dB
Expected direction	0 degree	Interference 3#direction	60 degree
Interference 1#direction	-40 degree	Interference 3#INR	20 dB

**FIGURE 4.** Normalized beam patterns under different SNR under mismatch error.

4. SIMULATION RESULT ANALYSIS

In this paper, MATLAB platform is used for simulation. Assume that the array signal receiving model is shown in Table 1. Aiming at DOA mismatch and element position error, the SGSC algorithm proposed in this paper is compared with Capon algorithm, GSC algorithm, and SQP algorithm (Capon-SQP algorithm based on Capon and stepwise quadratic programming), and the experimental analysis is given.

4.1. DOA Mismatch

4.1.1. Directional Diagram

When the DOA of the expected signal is mismatched and the mismatch error angle fixed at 2° , that is, the actual direction of arrival of the expected signal is 2° , the normalized beam patterns with Signal-to-Noise Ratio (SNR) of 0 dB and 10 dB respectively are shown in Fig. 4.

As can be seen from Fig. 4, due to the mismatch error, the main beams of Capon algorithm, GSC algorithm, and SQP algorithm are off-pointing, which cannot point to the desired signal direction correctly; nulls are also formed in other directions except the interference direction; and the pointing is unclear. Due to the correction of the steering vector, the main beam is formed by SGSC algorithm points to 2° with no deviation; the algorithm only forms null in the interference direction; and the

depth of null is below -50 dB. Therefore, the algorithm has good beam directivity and anti-jamming ability.

4.1.2. Different SNR

Assuming that the expected signal DOA is mismatched, and the mismatch error angles are fixed at 2° , 4° , -2° respectively, the actual expected signal arrival directions are 2° , 4° , -2° , respectively. Fig. 5, Fig. 6, and Fig. 7 are the output signal to interference plus noise ratio (SINR) curves of the algorithm under different SNRs under these three DOA mismatches. It can be seen from the figure that the main beams of Capon algorithm, GSC algorithm, and SQP algorithm cannot aim at the expected signal because of the mismatch error, which leads to the suppression of the expected signal, and the algorithm has no ability to counter the expected signal, so with the increase of SNR, the SINR output of the algorithm is lower. SGSC algorithm corrects the steering vector, and the sensitivity of the algorithm to mismatch error decreases. With the increase of SNR, the output SINR of SGSC algorithm gradually increases.

4.1.3. Different Mismatch Errors

Figure 8 shows the output SINR curves of the algorithm when SNR is 0 dB and 10 dB, respectively, and the mismatch error of the direction of arrival of the expected signal is between $[-5^\circ, 5^\circ]$.

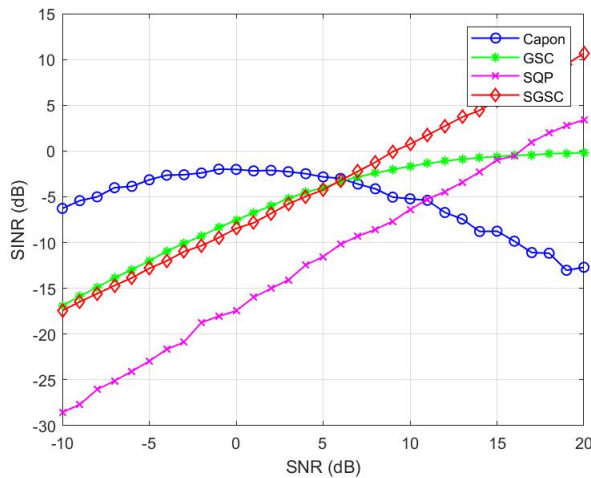


FIGURE 5. SINR curves of the algorithm under different SNR when the mismatch error is 2° .

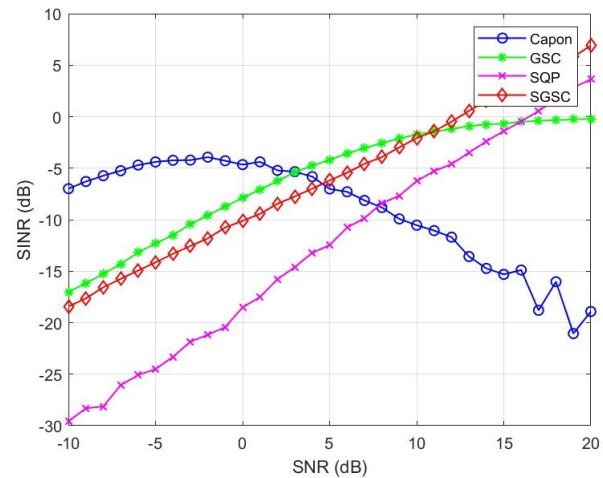


FIGURE 6. SINR curves of the algorithm under different SNR when the mismatch error is 4° .

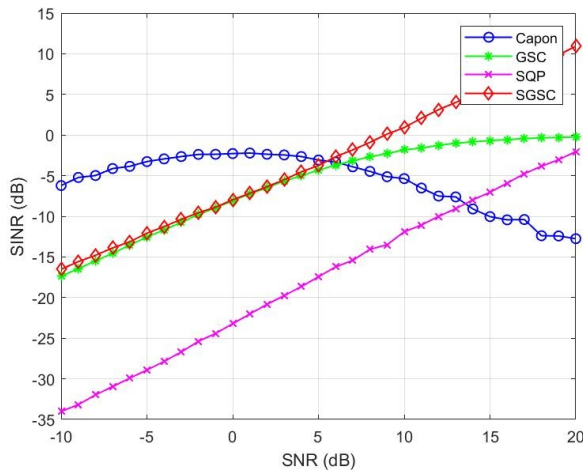


FIGURE 7. SINR curves of the algorithm under different SNR when the mismatch error is -2° .

As can be seen from the figure, when the mismatch error angle is 0° , that is, there is no mismatch, the output SINR of Capon algorithm, GSC algorithm, and SQP algorithm reaches the peak, but at other angles, the SINR of these three algorithms is unstable. With the increase of mismatch error angle, the performance becomes worse. Moreover, GSC algorithm, like Capon algorithm, has no robustness against steering vector mismatch because it does not correct the steering vector. Because SGSC algorithm corrects the steering vector, the SINR of its output is always stable and does not change with the change of mismatch error angle.

4.1.4. Different Snapshot Numbers

When the expected signal DOA is mismatched, if the mismatch error angle is fixed at 2° , the actual direction of arrival of the expected signal is 2° . Fig. 9 shows the curves of the output

SINR of the algorithm with the number of snapshots when SNR is 0 dB and 10 dB, respectively.

It can be seen from the figure that within 500 snapshots, Capon algorithm, GSC algorithm, and SQP algorithm suppress the expected signal due to the mismatch of steering vectors, which makes the output SINR loss serious, while SGSC algorithm has better output SINR due to the correction of steering vectors.

4.2. Array Element Position Error

4.2.1. Directional Diagram

It is assumed that the error of the real array element position and the error of the ideal array element position obey the random distribution on $[-0.1\lambda, 0.1\lambda]$, and the arrival direction of the expected signal is 0° .

When there is an element position error, the normalized beam pattern with SNR of 0 dB and 10 dB respectively is shown in Fig. 10. As can be seen from the figure, due to the position error of the array elements, the main beams of Capon algorithm, GSC algorithm, and SQP algorithm are deviated, and the direction of interference nulling is unclear. Due to the correction of the steering vector, the main beam formed by SGSC algorithm is 0° with no deviation; the algorithm only forms null in the interference direction; and the depth of null is below -50 dB. Therefore, the algorithm has good beam directivity and anti-jamming ability.

4.2.2. Different SNRs

It is assumed that the error of the real array element position and the error of the ideal array element position obey the random distribution on $[-0.1\lambda, 0.1\lambda]$, and the arrival direction of the expected signal is 0° . Fig. 11 is the output SINR curve of the algorithm under different SNRs when the position of the array element is wrong. It can be seen from the figure that the main beams of Capon algorithm, GSC algorithm, and SQP algorithm

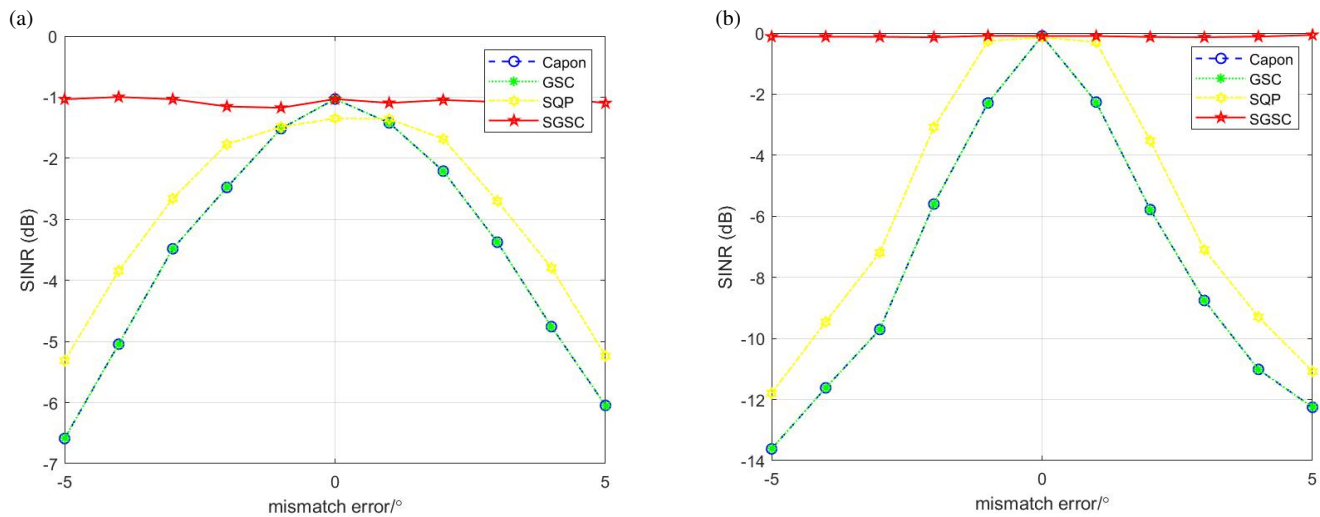


FIGURE 8. SINR output of the algorithm under different mismatch errors. (a) SNR = 0 dB. (b) SNR = 10 dB.

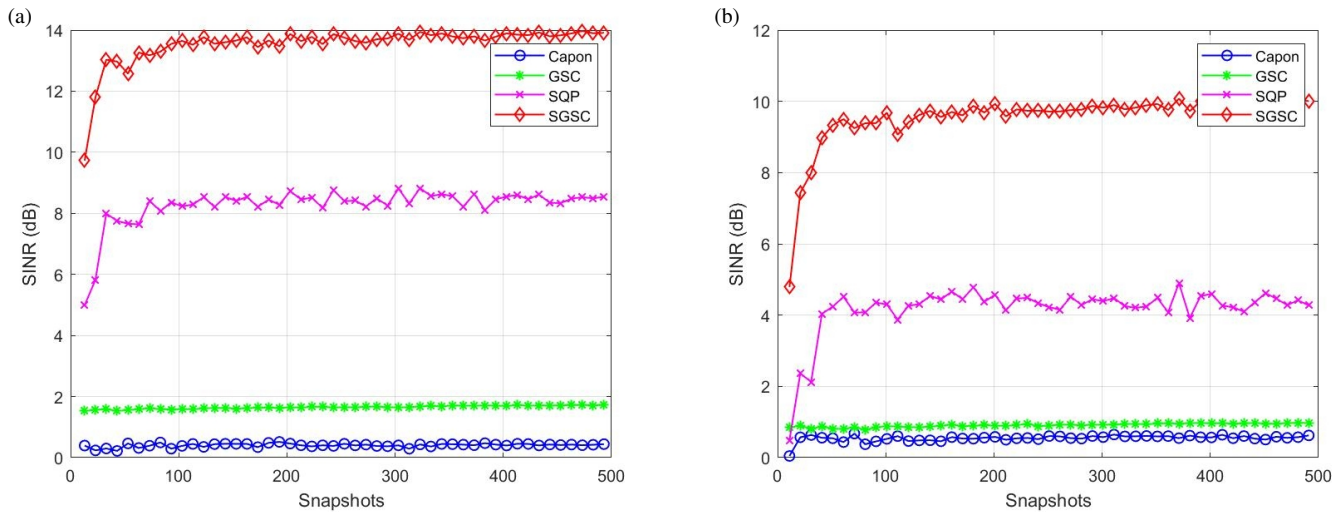


FIGURE 9. SINR curve of algorithm output under different snapshot numbers under mismatch error. (a) SNR = 0 dB. (b) SNR = 10 dB.

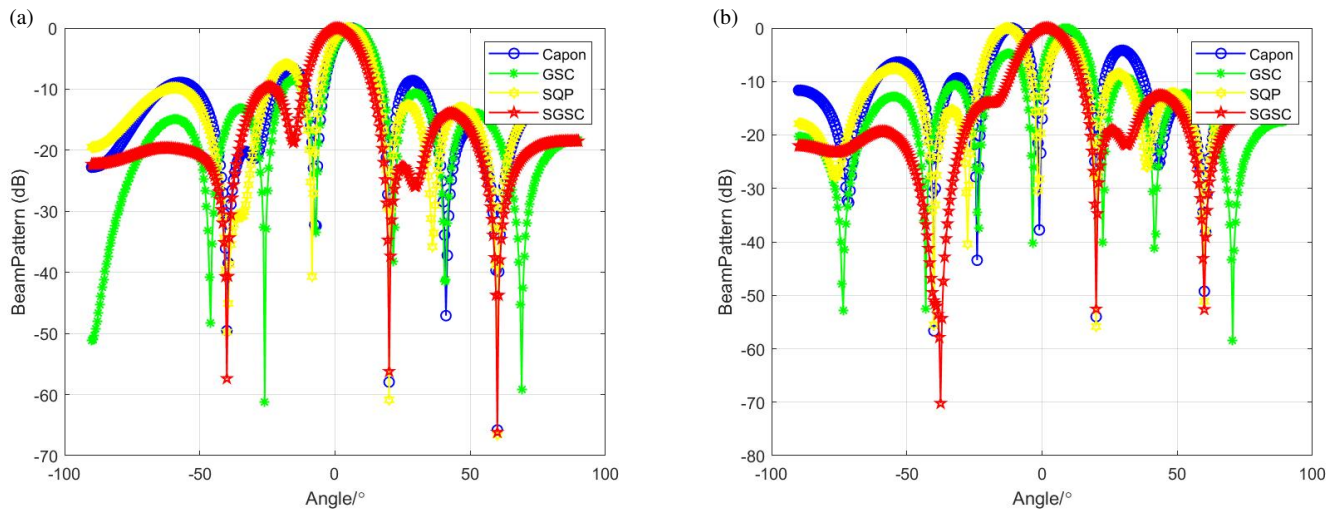


FIGURE 10. Normalized beam patterns with different SNR under array element position error. (a) SNR = 0 dB. (b) SNR = 10 dB.

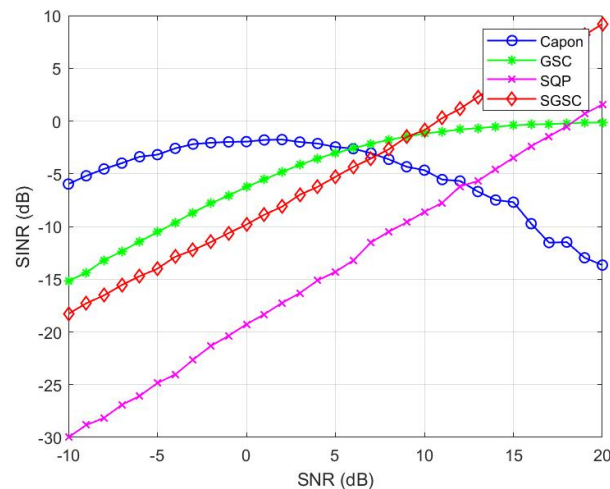


FIGURE 11. SINR curve of algorithm output under different SNR under array element position error.

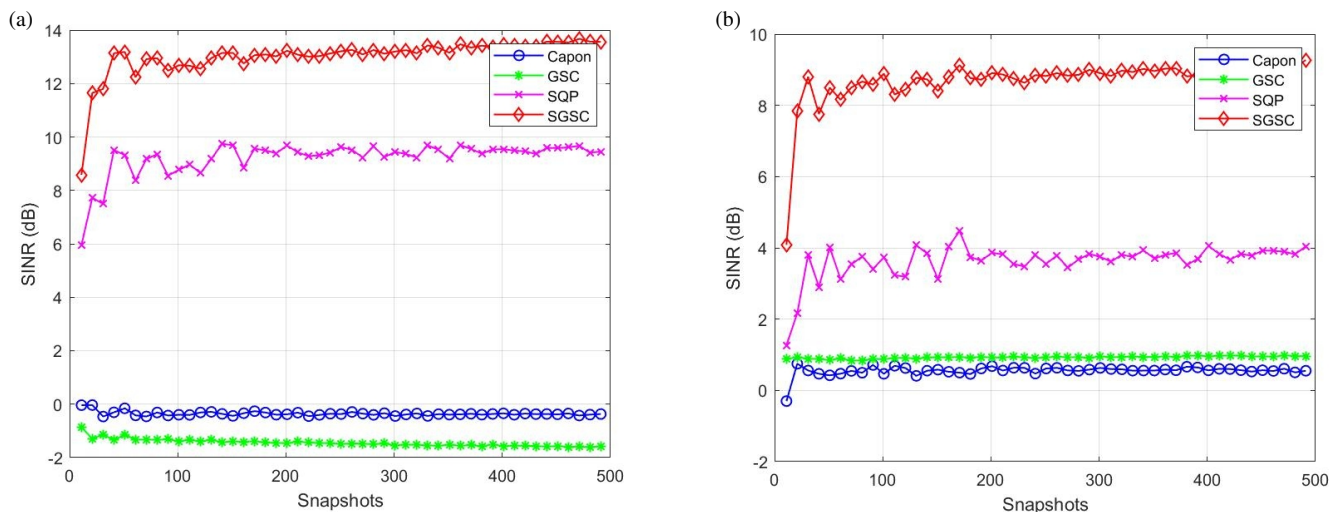


FIGURE 12. SINR curve of algorithm output under different snapshot numbers under array element position error. (a) SNR = 0 dB. (b) SNR = 10 dB.

cannot aim at the expected signal because of the position error of array elements, and the algorithm has no ability to counter the expected signal, so the SINR output of the algorithm does not increase obviously or even decreases with the increase of SNR. The sensitivity of SGSC algorithm to element position error decreases, and with the increase of SNR, the output SINR of SGSC algorithm increases gradually.

4.2.3. Different Snapshot Numbers

It is assumed that the error of the real array element position and the error of the ideal array element position obey the random distribution on $[-0.1\lambda, 0.1\lambda]$, and the arrival direction of the expected signal is 0° . Fig. 12 shows the curves of the output SINR of the algorithm with the number of snapshots when SNR is 0 dB and 10 dB, respectively. It can be seen from the figure that within 500 snapshots, Capon algorithm, GSC algorithm, and SQP algorithm suppress the expected signal due to the existence of array element position error, which makes the

output SINR loss serious, while SGSC algorithm has better output SINR due to the correction of steering vector.

4.3. Summarize and Analyze

In this paper, the steering vector of the expected signal and the weight vector of GSC are corrected by the method of stepwise quadratic programming, and a new SGSC algorithm is proposed. The algorithm is verified on the MATLAB simulation platform, and its robustness is analyzed from different aspects. In the case of DOA mismatch and element position error, the algorithm proposed in this paper can point to the direction of the desired signal without deviation from the normalized pattern and form a null in the interference direction and point clearly. Moreover, compared with other algorithms, the SINR of the algorithm proposed in this paper will gradually increase when different SNR is input, and the SINR is higher than that of other algorithms. According to the comparison chart of SINR output of the algorithm under different mismatch errors, it can be

seen that the algorithm proposed in this paper can make SINR unaffected by the angle of mismatch errors, thus proving the robustness of the algorithm.

5. CONCLUSIONS

Based on the conventional adaptive GSC algorithm, this paper proposes a new adaptive GSC algorithm. This method uses the stepwise quadratic algorithm to correct the steering vector of the expected signal, reduces the mismatch error between the assumed steering vector and the real steering vector, blocks the expected signal in the auxiliary antenna, corrects the weight vector of GSC algorithm, and effectively avoids the performance degradation of the algorithm caused by too large steering vector error. Compared with the conventional GSC algorithm, this algorithm is more robust when being applied to practical scenes.

REFERENCES

- [1] Wang, J. and K. Mouthaan, "Robust beamforming for antenna arrays with source location probability density function," in *2021 International Symposium on Antennas and Propagation (ISAP)*, 1–2, Taipei, Taiwan, 2021.
- [2] Nand, K., S. Agarwal, and G. Kaur, "Algorithms for adaptive beamforming in smart antenna in 5G," in *2023 3rd International Conference on Intelligent Technologies (CONIT)*, 1–6, Hubli, India, 2023.
- [3] Yang, H. and Z. Ye, "Robust adaptive beamforming based on covariance matrix reconstruction via steering vector estimation," *IEEE Sensors Journal*, Vol. 23, No. 3, 2932–2939, Feb. 2023.
- [4] Yazdi, N. and K. Todros, "Measure-transformed MVDR beamforming," *IEEE Signal Processing Letters*, Vol. 27, 1959–1963, 2020.
- [5] Zhu, X., X. Xu, and Z. Ye, "Robust adaptive beamforming via subspace for interference covariance matrix reconstruction," *Signal Processing*, Vol. 167, 107289, Feb. 2020.
- [6] Yuan, X. and L. Gan, "Robust adaptive beamforming via a novel subspace method for interference covariance matrix reconstruction," *Signal Processing*, Vol. 130, 233–242, Jan. 2017.
- [7] Zhu, X., Z. Ye, X. Xu, and R. Zheng, "Covariance matrix reconstruction via residual noise elimination and interference powers estimation for robust adaptive beamforming," *IEEE Access*, Vol. 7, 53 262–53 272, 2019.
- [8] Yang, H., P. Wang, and Z. Ye, "Robust adaptive beamforming via covariance matrix reconstruction and interference power estimation," *IEEE Communications Letters*, Vol. 25, No. 10, 3394–3397, Oct. 2021.
- [9] Lv, Y., F. Cao, J. Yang, C. He, X. Feng, and J. Xu, "Robust adaptive beamforming based on a novel covariance matrix selection strategy," in *2022 IEEE 5th International Conference on Electronics Technology (ICET)*, 680–684, Chengdu, China, 2022.
- [10] Li, Z., S. Cao, W. Zeng, and T. Li, "Robust beamforming algorithm based on steering vector estimation and interference plus noise covariance matrix reconstruction," in *2022 Signal Processing: Algorithms, Architectures, Arrangements, and Applications (SPA)*, 24–27, Poznan, Poland, 2022.
- [11] Li, L., R. Xu, and G. Li, "Robust adaptive beamforming based on generalized sidelobe cancellation," in *2006 CIE International Conference on Radar*, 1–4, Shanghai, China, 2006.
- [12] Liu, Z., S. Zhao, G. Zhang, and B. Jiao, "Robust adaptive beamforming for sidelobe canceller with null widening," *IEEE Sensors Journal*, Vol. 19, No. 23, 11 213–11 220, Dec. 2019.
- [13] Park, S., S. Jeong, M. Han, and S. Chi, "Performance improvement of GSC algorithms by near channel subtraction-based blocking matrix," in *2012 9th International Conference on Ubiquitous Robots and Ambient Intelligence (URAI)*, 633–635, Daejeon, South Korea, 2012.
- [14] Su, H. and C.-M. Lee, "Modified GSC method to reduce the distortion of the enhanced speech signal using cross-correlation and sidelobe neutralization," *Applied Sciences*, Vol. 11, No. 14, 6288, Jul. 2021.
- [15] Chang, J.-C., "A robust space-time generalized sidelobe canceller," *Wireless Personal Communications*, Vol. 70, 129–138, May 2013.
- [16] Yang, Q., Y. Zhou, Y. Ma, and H. Liu, "A new frequency-domain adaptive blocking matrix design for generalized sidelobe cancellation," in *2020 15th IEEE International Conference on Signal Processing (ICSP)*, Vol. 1, 109–113, Beijing, China, 2020.
- [17] Lin, X., Y. Huang, W. Yang, and J. Xu, "Robust adaptive beamforming with multiple signal mismatch constraints: A sequential convex approximation method," in *2023 31st European Signal Processing Conference (EUSIPCO)*, 1634–1638, Helsinki, Finland, 2023.
- [18] Wu, Z., S. Zhu, J. Xu, L. Lan, Y. Xu, X. Li, and J. Gao, "Robust adaptive beamforming based on MR-FDA-MIMO radar jamming suppression," in *2023 IEEE International Radar Conference (RADAR)*, 1–6, Sydney, Australia, 2023.
- [19] Huang, Y., H. Fu, S. A. Vorobyov, and Z.-Q. Luo, "Robust adaptive beamforming via worst-case SINR maximization with non-convex uncertainty sets," *IEEE Transactions on Signal Processing*, Vol. 71, 218–232, 2023.
- [20] Guo, J., H. Yang, and Z. Ye, "A novel robust adaptive beamforming algorithm based on subspace orthogonality and projection," *IEEE Sensors Journal*, Vol. 23, No. 11, 12 076–12 083, Jun. 2023.
- [21] Liu, Z., S. Wu, Y. Wang, W. Guo, and J. Zhang, "A new GSC beamforming algorithm based on double affine projection," in *2014 IEEE International Symposium on Broadband Multimedia Systems and Broadcasting*, 1–4, Beijing, China, 2014.
- [22] Dietzen, T., A. Spriet, W. Tirry, S. Doclo, M. Moonen, and T. van Waterschoot, "Comparative analysis of generalized sidelobe cancellation and multi-channel linear prediction for speech dereverberation and noise reduction," *IEEE/ACM Transactions on Audio, Speech, and Language Processing*, Vol. 27, No. 3, 544–558, Mar. 2019.